

# Production rate and decay lifetime measurements of $B_s^0$ mesons at LEP using $D_s$ and $\phi$ mesons

DELPHI Collaboration

P. Abreu<sup>20</sup>, W. Adam<sup>7</sup>, T. Adaye<sup>37</sup>, E. Agasi<sup>30</sup>, R. Aleksan<sup>39</sup>, G.D. Alekseev<sup>14</sup>, A. Algeri<sup>13</sup>, S. Almedhed<sup>23</sup>, S.J. Alvsvaag<sup>4</sup>, U. Amaldi<sup>7</sup>, A. Andreazza<sup>27</sup>, P. Antilogus<sup>24</sup>, W.-D. Apel<sup>15</sup>, R.J. Apsimon<sup>37</sup>, Y. Arnaud<sup>39</sup>, B. Åsman<sup>45</sup>, J.-E. Augustin<sup>18</sup>, A. Augustinus<sup>30</sup>, P. Baillon<sup>7</sup>, P. Bambade<sup>18</sup>, F. Barao<sup>20</sup>, R. Barate<sup>12</sup>, G. Barbiellini<sup>47</sup>, D.Y. Bardin<sup>14</sup>, G.J. Barker<sup>34</sup>, A. Baroncelli<sup>41</sup>, O. Barring<sup>7</sup>, J.A. Barrio<sup>25</sup>, M.J. Bates<sup>37</sup>, M. Battaglia<sup>13</sup>, M. Baubillier<sup>22</sup>, K.-H. Becks<sup>52</sup>, M. Begalli<sup>36</sup>, P. Beilliere<sup>6</sup>, Yu. Belokopytov<sup>43</sup>, P. Beltran<sup>9</sup>, D. Benedic<sup>8</sup>, A.C. Benvenuti<sup>5</sup>, M. Berggren<sup>18</sup>, D. Bertrand<sup>2</sup>, F. Bianchi<sup>46</sup>, M. Bigi<sup>46</sup>, M.S. Bilenky<sup>14</sup>, P. Billoir<sup>22</sup>, J. Bjarne<sup>23</sup>, D. Bloch<sup>8</sup>, J. Blocki<sup>51</sup>, S. Blyth<sup>34</sup>, V. Bocci<sup>38</sup>, P.N. Bogolubov<sup>14</sup>, T. Bolognese<sup>39</sup>, M. Bonesini<sup>27</sup>, W. Bonivento<sup>27</sup>, P.S.L. Booth<sup>21</sup>, G. Borisov<sup>43</sup>, H. Borner<sup>7</sup>, C. Bosio<sup>41</sup>, B. Bostjancic<sup>44</sup>, S. Bosworth<sup>34</sup>, O. Botner<sup>48</sup>, B. Bouquet<sup>18</sup>, C. Bourdarios<sup>18</sup>, T.J.V. Bowcock<sup>21</sup>, M. Bozzo<sup>11</sup>, S. Braibant<sup>2</sup>, P. Branchini<sup>41</sup>, K.D. Brand<sup>35</sup>, R.A. Brenner<sup>7</sup>, H. Briand<sup>22</sup>, C. Bricman<sup>2</sup>, L. Brillaut<sup>22</sup>, R.C.A. Brown<sup>7</sup>, J.-M. Brunet<sup>6</sup>, A. Budziak<sup>16</sup>, L. Bugge<sup>32</sup>, T. Buran<sup>32</sup>, H. Burmeister<sup>7</sup>, A. Buys<sup>7</sup>, J.A.M.A. Buytaert<sup>7</sup>, M. Caccia<sup>7</sup>, M. Calvi<sup>27</sup>, A.J. Camacho Rozas<sup>42</sup>, R. Campion<sup>21</sup>, T. Camporesi<sup>7</sup>, V. Canale<sup>38</sup>, K. Cankocak<sup>45</sup>, F. Cao<sup>2</sup>, F. Carena<sup>7</sup>, L. Carroll<sup>21</sup>, C. Caso<sup>11</sup>, M.V. Castillo Gimenez<sup>49</sup>, A. Cattai<sup>7</sup>, F.R. Cavallo<sup>5</sup>, L. Cerrito<sup>38</sup>, V. Chabaud<sup>7</sup>, A. Chan<sup>1</sup>, M. Chapkin<sup>43</sup>, Ph. Charpentier<sup>7</sup>, L. Chaussard<sup>18</sup>, J. Chauveau<sup>22</sup>, P. Checchia<sup>35</sup>, G.A. Chelkov<sup>14</sup>, L. Chevalier<sup>39</sup>, P. Chliapnikov<sup>43</sup>, V. Chorowicz<sup>22</sup>, J.T.M. Chrin<sup>49</sup>, V. Cindro<sup>44</sup>, P. Collins<sup>34</sup>, J.L. Contreras<sup>25</sup>, R. Contri<sup>11</sup>, E. Cortina<sup>49</sup>, G. Cosme<sup>18</sup>, F. Couchot<sup>18</sup>, H.B. Crawley<sup>1</sup>, D. Crennell<sup>37</sup>, G. Crosetti<sup>11</sup>, J. Cuevas Maestro<sup>33</sup>, S. Czellar<sup>13</sup>, E. Dahl-Jensen<sup>28</sup>, J. Dahm<sup>52</sup>, B. Dalmagne<sup>18</sup>, M. Dam<sup>32</sup>, G. Damgaard<sup>28</sup>, E. Daubie<sup>2</sup>, A. Daum<sup>15</sup>, P.D. Dauncey<sup>34</sup>, M. Davenport<sup>7</sup>, J. Davies<sup>21</sup>, W. Da Silva<sup>22</sup>, C. Defoix<sup>6</sup>, P. Delpierre<sup>26</sup>, N. Demaria<sup>46</sup>, A. De Angelis<sup>47</sup>, H. De Boeck<sup>2</sup>, W. De Boer<sup>15</sup>, S. De Brabandere<sup>2</sup>, C. De Clerq<sup>2</sup>, M.D.M. De Fez Laso<sup>49</sup>, C. De La Vaissiere<sup>22</sup>, B. De Lotto<sup>47</sup>, A. De Min<sup>27</sup>, H. Dijkstra<sup>7</sup>, L. Di Ciaccio<sup>38</sup>, J. Dolbeau<sup>6</sup>, M. Donszelmann<sup>7</sup>, K. Doroba<sup>51</sup>, M. Dracos<sup>7</sup>, J. Drees<sup>52</sup>, M. Dris<sup>31</sup>, Y. Dufour<sup>7</sup>, F. Dupont<sup>7</sup>, D. Edsall<sup>12</sup>, L.-O. Eek<sup>48</sup>, P.A.-M. Eerola<sup>7</sup>, R. Ehret<sup>15</sup>, T. Ekelof<sup>48</sup>, G. Ekspong<sup>45</sup>, A. Elliot Peisert<sup>35</sup>, M. Elsing<sup>52</sup>, J.-P. Engel<sup>8</sup>, N. Ershaidat<sup>22</sup>, M. Espirito Santo<sup>20</sup>, D. Fassouliotis<sup>31</sup>, M. Feindt<sup>7</sup>, A. Ferrer<sup>49</sup>, T.A. Filippas<sup>31</sup>, A. Firestone<sup>1</sup>, H. Foeth<sup>7</sup>, E. Fokitis<sup>31</sup>, F. Fontanelli<sup>11</sup>, K.A.J. Forbes<sup>21</sup>, J.-L. Fousset<sup>26</sup>, S. Francon<sup>24</sup>, B. Franek<sup>37</sup>, P. Frenkiel<sup>6</sup>, D.C. Fries<sup>15</sup>, A.G. Frodesen<sup>4</sup>, R. Fruhwirth<sup>50</sup>, F. Fulda-Quenzer<sup>18</sup>, H. Furstenuau<sup>15</sup>, J. Fuster<sup>7</sup>, D. Gamba<sup>46</sup>, C. Garcia<sup>49</sup>, J. Garcia<sup>42</sup>, C. Gaspar<sup>7</sup>, U. Gasparini<sup>35</sup>, Ph. Gavillet<sup>7</sup>, E.N. Gazis<sup>31</sup>, J.-P. Gerber<sup>8</sup>, P. Giacomelli<sup>7</sup>, D. Gillespie<sup>7</sup>, R. Gokiel<sup>51</sup>, B. Golob<sup>44</sup>, V.M. Golovatyuk<sup>14</sup>, J.J. Gomez Y Cadenas<sup>7</sup>, G. Gopal<sup>37</sup>, L. Gorn<sup>1</sup>, M. Gorski<sup>51</sup>, V. Gracco<sup>11</sup>, A. Grant<sup>7</sup>, F. Grand<sup>2</sup>, E. Graziani<sup>41</sup>, G. Grosdidier<sup>18</sup>, E. Gross<sup>7</sup>, B. Grossetete<sup>22</sup>, P. Gunnarsson<sup>45</sup>, J. Guy<sup>37</sup>, U. Haedinger<sup>15</sup>, F. Hahn<sup>52</sup>, M. Hahn<sup>45</sup>, S. Hahn<sup>52</sup>, S. Haider<sup>30</sup>, Z. Hajduk<sup>16</sup>, A. Hakansson<sup>23</sup>, A. Hallgren<sup>48</sup>, K. Hamacher<sup>52</sup>, G. Hamel De Monchenault<sup>39</sup>, W. Hao<sup>30</sup>, F.J. Harris<sup>34</sup>, V. Hedberg<sup>23</sup>, T. Henkes<sup>7</sup>, R. Henriques<sup>20</sup>, J.J. Hernandez<sup>49</sup>, J.A. Hernandez<sup>49</sup>, P. Herquet<sup>2</sup>, H. Herr<sup>7</sup>, T.L. Hessing<sup>21</sup>, I. Hietanen<sup>13</sup>, C.O. Higgins<sup>21</sup>, E. Higon<sup>49</sup>, H.J. Hilke<sup>7</sup>, T.S. Hill<sup>1</sup>, S.D. Hodgson<sup>34</sup>, T. Hofmökler<sup>51</sup>, S.-O. Holmgren<sup>45</sup>, P.J. Holt<sup>34</sup>, D. Holthuisen<sup>30</sup>, P.F. Honore<sup>6</sup>, M. Houlden<sup>21</sup>, J. Hrubec<sup>50</sup>, K. Huet<sup>2</sup>, K. Hultqvist<sup>45</sup>, P. Ioannou<sup>3</sup>, P.-S. Iversen<sup>4</sup>, J.N. Jackson<sup>21</sup>, R. Jacobsson<sup>45</sup>, P. Jalocho<sup>16</sup>, G. Jarlskog<sup>23</sup>, P. Jarry<sup>39</sup>, B. Jean-Marie<sup>18</sup>, E.K. Johansson<sup>45</sup>, M. Jonker<sup>7</sup>, L. Jonsson<sup>23</sup>, P. Juillot<sup>8</sup>, G. Kalkanis<sup>3</sup>, G. Kalmus<sup>37</sup>, F. Kapusta<sup>22</sup>, M. Karlsson<sup>45</sup>, E. Karvelas<sup>9</sup>, S. Katsanevas<sup>3</sup>, E.C. Katsoufis<sup>31</sup>, R. Keranen<sup>7</sup>, B.A. Khomenko<sup>14</sup>, N.N. Khovanski<sup>14</sup>, B. King<sup>21</sup>, N.J. Kjaer<sup>7</sup>, H. Klein<sup>7</sup>, A. Klovning<sup>4</sup>, P. Kluit<sup>30</sup>, A. Koch-Mehrin<sup>52</sup>, J.H. Koehne<sup>15</sup>, B. Koene<sup>30</sup>, P. Kokkinias<sup>9</sup>, M. Koratzinos<sup>32</sup>, K. Korcyl<sup>16</sup>, A.V. Korytov<sup>14</sup>, V. Kostioukhine<sup>43</sup>, C. Kourkoumelis<sup>3</sup>, O. Kouznetsov<sup>14</sup>, P.H. Kramer<sup>52</sup>, M. Krammer<sup>50</sup>, C. Kreuter<sup>15</sup>, J. Krolikowski<sup>51</sup>, I. Kronkvist<sup>23</sup>, W. Kucewicz<sup>16</sup>, K. Kulka<sup>48</sup>, K. Kurvinen<sup>13</sup>, C. Lacasta<sup>49</sup>, C. Lambropoulos<sup>9</sup>, J.W. Lamsa<sup>1</sup>, L. Lancieri<sup>47</sup>, P. Langefeld<sup>52</sup>, V. Lapin<sup>43</sup>, I. Last<sup>21</sup>, J.-P. Laugier<sup>39</sup>, R. Lauhakangas<sup>13</sup>, G. Leder<sup>50</sup>, F. Ledroit<sup>12</sup>, R. Leitner<sup>29</sup>, Y. Lemoigne<sup>39</sup>, J. Lemonne<sup>2</sup>, G. Lenzen<sup>52</sup>, V. Lepeltier<sup>18</sup>, T. Lesiak<sup>16</sup>, J.M. Levy<sup>8</sup>, E. Lieb<sup>52</sup>, D. Liko<sup>50</sup>, J. Lindgren<sup>13</sup>, R. Lindner<sup>52</sup>, I. Lippi<sup>35</sup>, B. Loerstad<sup>23</sup>, M. Lokajicek<sup>10</sup>, J.G. Loken<sup>34</sup>,

A. Lopez-Fernandez<sup>7</sup>, M.A. Lopez Aguera<sup>42</sup>, M. Los<sup>30</sup>, D. Loukas<sup>9</sup>, J.J. Lozano<sup>49</sup>, P. Lutz<sup>6</sup>, L. Lyons<sup>34</sup>, G. Maehlum<sup>32</sup>, J. Maillard<sup>6</sup>, A. Maio<sup>20</sup>, A. Maltezos<sup>9</sup>, F. Mandl<sup>50</sup>, J. Marco<sup>42</sup>, M. Margoni<sup>35</sup>, J.-C. Marin<sup>7</sup>, A. Markou<sup>9</sup>, T. Maron<sup>52</sup>, S. Marti<sup>49</sup>, C. Martinez-Rivero<sup>42</sup>, F. Martinez-Vidal<sup>49</sup>, F. Matorras<sup>42</sup>, C. Matteuzzi<sup>27</sup>, G. Matthiae<sup>38</sup>, M. Mazzucato<sup>35</sup>, M. Mc Cubbin<sup>21</sup>, R. Mc Kay<sup>1</sup>, R. Mc Nulty<sup>21</sup>, J. Medbo<sup>48</sup>, C. Meroni<sup>27</sup>, W.T. Meyer<sup>1</sup>, M. Michelotto<sup>35</sup>, I. Mikulec<sup>50</sup>, L. Mirabito<sup>24</sup>, W.A. Mitaroff<sup>50</sup>, G.V. Mitselmakher<sup>14</sup>, U. Mjoernmark<sup>23</sup>, T. Moa<sup>45</sup>, R. Moeller<sup>28</sup>, K. Moenig<sup>7</sup>, M.R. Monge<sup>11</sup>, P. Morettini<sup>11</sup>, H. Mueller<sup>15</sup>, W.J. Murray<sup>37</sup>, G. Myatt<sup>34</sup>, F.L. Navarria<sup>5</sup>, P. Negri<sup>27</sup>, S. Nemecek<sup>10</sup>, W. Neumann<sup>52</sup>, R. Nicolaidou<sup>3</sup>, B.S. Nielsen<sup>28</sup>, B. Nijhar<sup>21</sup>, V. Nikolaenko<sup>43</sup>, P.E.S. Nilsen<sup>4</sup>, P. Niss<sup>45</sup>, A. Nomerotski<sup>35</sup>, V. Obraztsov<sup>43</sup>, A.G. Olshevski<sup>14</sup>, R. Orava<sup>13</sup>, A. Ostankov<sup>43</sup>, K. Osterberg<sup>13</sup>, A. Ouraou<sup>39</sup>, M. Paganoni<sup>27</sup>, R. Pain<sup>22</sup>, H. Palka<sup>16</sup>, Th.D. Papadopoulou<sup>31</sup>, L. Pape<sup>7</sup>, F. Parodi<sup>11</sup>, A. Passeri<sup>41</sup>, M. Pegoraro<sup>35</sup>, J. Pennanen<sup>13</sup>, L. Peralta<sup>20</sup>, V. Perevozchikov<sup>43</sup>, H. Pernegger<sup>50</sup>, M. Pernicka<sup>50</sup>, A. Perrotta<sup>5</sup>, C. Petridou<sup>47</sup>, A. Petrolini<sup>11</sup>, G. Piana<sup>11</sup>, F. Pierre<sup>39</sup>, M. Pimenta<sup>20</sup>, S. Plaszczynski<sup>18</sup>, O. Podobrin<sup>15</sup>, M.E. Pol<sup>17</sup>, G. Polok<sup>16</sup>, P. Poropat<sup>47</sup>, V. Pozdniakov<sup>14</sup>, P. Privitera<sup>38</sup>, A. Pullia<sup>27</sup>, D. Radojicic<sup>34</sup>, S. Ragazzi<sup>27</sup>, H. Rahmani<sup>31</sup>, J. Rames<sup>10</sup>, P.N. Ratoff<sup>19</sup>, A.L. Read<sup>32</sup>, M. Reale<sup>52</sup>, P. Rebecchi<sup>7</sup>, N.G. Redaelli<sup>27</sup>, M. Regler<sup>50</sup>, D. Reid<sup>7</sup>, P.B. Renton<sup>34</sup>, L.K. Resvanis<sup>3</sup>, F. Richard<sup>18</sup>, J. Richardson<sup>21</sup>, J. Ridky<sup>10</sup>, G. Rinaudo<sup>46</sup>, I. Roditi<sup>17</sup>, A. Romero<sup>46</sup>, I. Roncagliolo<sup>11</sup>, P. Ronchese<sup>35</sup>, C. Ronnqvist<sup>13</sup>, E.I. Rosenberg<sup>1</sup>, E. Rosso<sup>7</sup>, T. Rovelli<sup>5</sup>, W. Ruckstuhl<sup>30</sup>, V. Ruhlmann-Kleider<sup>39</sup>, A. Ruiz<sup>42</sup>, H. Saarikko<sup>13</sup>, Y. Sacquin<sup>39</sup>, G. Sajot<sup>12</sup>, J. Salt<sup>49</sup>, J. Sanchez<sup>25</sup>, M. Sannino<sup>11,40</sup>, S. Schael<sup>7</sup>, H. Schneider<sup>15</sup>, M.A.E. Schyns<sup>52</sup>, G. Sciolla<sup>46</sup>, F. Scuri<sup>47</sup>, A.M. Segar<sup>34</sup>, A. Seitz<sup>15</sup>, R. Sekulin<sup>37</sup>, M. Sessa<sup>47</sup>, R. Seufert<sup>15</sup>, R.C. Shellard<sup>36</sup>, I. Siccama<sup>30</sup>, P. Siegrist<sup>39</sup>, S. Simonetti<sup>11</sup>, F. Simonetto<sup>35</sup>, A.N. Sisakian<sup>14</sup>, G. Skjevling<sup>32</sup>, G. Smadja<sup>39,24</sup>, N. Smirnov<sup>43</sup>, O. Smirnova<sup>14</sup>, G.R. Smith<sup>37</sup>, R. Sosnowski<sup>51</sup>, D. Souza-Santos<sup>36</sup>, T. Spassoff<sup>20</sup>, E. Spiriti<sup>41</sup>, S. Squarcia<sup>11</sup>, H. Staeck<sup>52</sup>, C. Stanescu<sup>41</sup>, S. Stapes<sup>32</sup>, G. Stavropoulos<sup>9</sup>, F. Stichelbaut<sup>2</sup>, A. Stocchi<sup>18</sup>, J. Strauss<sup>50</sup>, J. Straver<sup>7</sup>, R. Strub<sup>8</sup>, B. Stugu<sup>4</sup>, M. Szczekowski<sup>7</sup>, M. Szeptycka<sup>51</sup>, P. Szymanski<sup>51</sup>, T. Tabarelli<sup>27</sup>, O. Tchikilev<sup>43</sup>, G.E. Theodosiou<sup>9</sup>, A. Tilquin<sup>26</sup>, J. Timmermans<sup>30</sup>, V.G. Timofeev<sup>14</sup>, L.G. Tkatchev<sup>14</sup>, T. Todorov<sup>8</sup>, D.Z. Toet<sup>30</sup>, O. Toker<sup>13</sup>, A. Tomaradze<sup>2</sup>, B. Tome<sup>20</sup>, E. Torassa<sup>46</sup>, L. Tortora<sup>41</sup>, D. Treille<sup>7</sup>, W. Trischuk<sup>7</sup>, G. Tristram<sup>6</sup>, C. Troncon<sup>27</sup>, A. Tsirou<sup>7</sup>, E.N. Tsyganov<sup>14</sup>, M.-L. Turluer<sup>39</sup>, T. Tuuva<sup>13</sup>, I.A. Tyapkin<sup>22</sup>, M. Tyndel<sup>37</sup>, S. Tzamarias<sup>21</sup>, B. Ueberschaer<sup>52</sup>, S. Ueberschaer<sup>52</sup>, O. Ullaland<sup>7</sup>, V. Uvarov<sup>43</sup>, G. Valenti<sup>5</sup>, E. Vallazza<sup>7</sup>, J.A. Valls Ferrer<sup>49</sup>, C. Vander Velde<sup>2</sup>, G.W. Van Apeldoorn<sup>30</sup>, P. Van Dam<sup>30</sup>, M. Van Der Heijden<sup>30</sup>, W.K. Van Doninck<sup>2</sup>, J. Van Eldik<sup>30</sup>, P. Vaz<sup>7</sup>, G. Vegni<sup>27</sup>, L. Ventura<sup>35</sup>, W. Venus<sup>37</sup>, F. Verbeure<sup>2</sup>, M. Verlati<sup>35</sup>, L.S. Vertogradov<sup>14</sup>, D. Vilanova<sup>39</sup>, P. Vincent<sup>24</sup>, L. Vitale<sup>13</sup>, E. Vlasov<sup>43</sup>, A.S. Vodopyanov<sup>14</sup>, M. Vollmer<sup>52</sup>, M. Voutilainen<sup>13</sup>, V. Vrba<sup>41</sup>, H. Wahlen<sup>52</sup>, C. Walck<sup>45</sup>, F. Waldner<sup>47</sup>, A. Wehr<sup>52</sup>, M. Weierstall<sup>52</sup>, P. Weilhammer<sup>7</sup>, A.M. Wetherell<sup>7</sup>, J.H. Wickens<sup>2</sup>, M. Wielers<sup>15</sup>, G.R. Wilkinson<sup>34</sup>, W.S.C. Williams<sup>34</sup>, M. Winter<sup>8</sup>, M. Witek<sup>16</sup>, G. Wormser<sup>18</sup>, K. Woschnagg<sup>48</sup>, A. Zaitsev<sup>43</sup>, A. Zalewska<sup>16</sup>, P. Zalewski<sup>18</sup>, D. Zavrtanik<sup>44</sup>, E. Zevgolatakos<sup>9</sup>, N.I. Zimin<sup>14</sup>, M. Zito<sup>39</sup>, D. Zontar<sup>44</sup>, R. Zuberi<sup>34</sup>, G. Zumerle<sup>35</sup>, J. Zuniga<sup>49</sup>

<sup>1</sup> Ames Laboratory and Department of Physics, Iowa State University, Ames, IA 50011, USA

<sup>2</sup> Physics Department, Univ. Instelling Antwerpen, Universiteitsplein 1, B-2610 Wilrijk, Belgium, and IIHE, ULB-VUB, Pleinlaan 2, B-1050 Brussels, Belgium, and Faculté des Sciences, Univ. de l'Etat Mons, Av. Maistriau 19, B-7000 Mons, Belgium

<sup>3</sup> Physics Laboratory, University of Athens, Solonos Str. 104, GR-10680 Athens, Greece

<sup>4</sup> Department of Physics, University of Bergen, Allégaten 55, N-5007 Bergen, Norway

<sup>5</sup> Dipartimento di Fisica, Università di Bologna and INFN, Via Irnerio 46, I-40126 Bologna, Italy

<sup>6</sup> Collège de France, Lab. de Physique Corpusculaire, IN2P3-CNRS, F-75231 Paris Cedex 05, France

<sup>7</sup> CERN, CH-1211 Geneva 23, Switzerland

<sup>8</sup> Centre de Recherche Nucléaire, IN2P3, CNRS/ULP, BP20, F-67037 Strasbourg Cedex, France

<sup>9</sup> Institute of Nuclear Physics, N.C.S.R. Demokritos, P.O. Box 60228, GR-15310 Athens, Greece

<sup>10</sup> FZU, Inst. of Physics of the C.A.S. High Energy Physics Division, Na Slovance 2, CS-180 40, Praha 8, Czechoslovakia

<sup>11</sup> Dipartimento di Fisica, Università di Genova and INFN, Via Dodecaneso 33, I-16146 Genova, Italy

<sup>12</sup> Institut des Sciences Nucléaires, IN2P3-CNRS, Université de Grenoble 1, F-38026 Grenoble, France

<sup>13</sup> Research Institute for High Energy Physics, SEFT, P.O. Box 9, FIN-00014 University of Helsinki, Finland

<sup>14</sup> Joint Institute for Nuclear Research, Dubna, Head Post Office, P.O. Box 79, 101 000 Moscow, Russia

<sup>15</sup> Institut für Experimentelle Kernphysik, Universität Karlsruhe, Postfach 6980, D-76128 Karlsruhe, Germany

<sup>16</sup> High Energy Physics Laboratory, Institute of Nuclear Physics, Ul. Kawory 26a, PL-30055 Krakow 30, Poland

<sup>17</sup> Centro Brasileiro de Pesquisas Físicas, rua Xavier Sigaud 150, RJ-22290 Rio de Janeiro, Brazil

<sup>18</sup> Université de Paris-Sud, Lab. de l'Accélérateur Linéaire, IN2P3-CNRS, Bat 200, F-91405 Orsay, France

<sup>19</sup> School of Physics and Materials, University of Lancaster, Lancaster LA1 4YB, UK

<sup>20</sup> LIP, IST, FCUL, Av. Elias Garcia, 14, 1º, P-1000 Lisboa Codex, Portugal

<sup>21</sup> Department of Physics, University of Liverpool, P.O. Box 147, Liverpool L69 3BX, UK

<sup>22</sup> LPNHE, IN2P3-CNRS, Universités Paris VI et VII, Tour 33 (RdC), 4 place Jussieu, F-75252 Paris Cedex 05, France

<sup>23</sup> Department of Physics, University of Lund, Sölvegatan 14, S-22363 Lund, Sweden

<sup>24</sup> Université Claude Bernard de Lyon, IPNL, IN2P3-CNRS, F-69622 Villeurbanne Cedex, France

<sup>25</sup> Universidad Complutense, Avda. Complutense s/n, E-28040 Madrid, Spain

<sup>26</sup> Univ. d'Aix, Marseille II, CPP, IN2P3-CNRS, F-13288 Marseille Cedex 09, France

<sup>27</sup> Dipartimento di Fisica, Università di Milano and INFN, Via Celoria 16, I-20133 Milan, Italy

<sup>28</sup> Niels Bohr Institute, Blegdamsvej 17, DK-2100 Copenhagen O, Denmark

<sup>29</sup> NC, Nuclear Centre of MFF, Charles University, Areal MFF, V Holešovičkách 2, CS-180 00, Praha 8, Czechoslovakia

<sup>30</sup> NIKHEF-H, Postbus 41882, 1009 DB Amsterdam, The Netherlands

- <sup>31</sup> National Technical University, Physics Department, Zografou Campus, GR-15773 Athens, Greece  
<sup>32</sup> Physics Department, University of Oslo, Blindern, N-1000 Oslo 3, Norway  
<sup>33</sup> Dpto. Fisica, Univ. Oviedo, C/P. Jimenez Casas, S/N, E-33006 Oviedo, Spain  
<sup>34</sup> Department of Physics, University of Oxford, Keble Road, Oxford OX1 3RH, UK  
<sup>35</sup> Dipartimento di Fisica, Università di Padova and INFN, Via Marzolo 8, I-35131 Padua, Italy  
<sup>36</sup> Depto. de Fisica, Pontificia Univ. Católica, C.P. 38071, RJ-22453 Rio de Janeiro, Brazil  
<sup>37</sup> Rutherford Appleton Laboratory, Chilton, Didcot OX11 0QX, UK  
<sup>38</sup> Dipartimento di Fisica, Università di Roma II and INFN, Tor Vergata, I-00173 Rome, Italy  
<sup>39</sup> Centre d'Etude de Saclay, DSM/DAPNIA, F-91191 Gif-sur-Yvette Cedex, France  
<sup>40</sup> Dipartimento di Fisica, Università di Salerno, I-84100 Salerno, Italy  
<sup>41</sup> Istituto Superiore di Sanità, Ist. Naz. di Fisica Nucl. (INFN), Viale Regina Elena 299, I-00161 Rome, Italy  
<sup>42</sup> C.E.A.F.M., C.S.I.C., Univ. Cantabria, Avda. los Castros, S/N, E-39006 Santander, Spain  
<sup>43</sup> Inst. for High Energy Physics, Serpukov P.O. Box 35, Protvino, (Moscow Region), Russia  
<sup>44</sup> J. Stefan Institute and Department of Physics, University of Ljubljana, Jamova 39, SI-61000 Ljubljana, Slovenia  
<sup>45</sup> Fysikum, Stockholm University, Box 6730, S-113 85 Stockholm, Sweden  
<sup>46</sup> Dipartimento di Fisica Sperimentale, Università di Torino and INFN, Via P. Giuria 1, I-10125 Turin, Italy  
<sup>47</sup> Dipartimento di Fisica, Università di Trieste and INFN, Via A. Valerio 2, I-34127 Trieste, Italy and Istituto di Fisica, Università di Udine, I-33100 Udine, Italy  
<sup>48</sup> Department of Radiation Sciences, University of Uppsala, P.O. Box 535, S-751 21 Uppsala, Sweden  
<sup>49</sup> IFIC, Valencia-CSIC, and D.F.A.M.N., U. de Valencia, Avda. Dr. Moliner 50, E-46100 Burjassot (Valencia), Spain  
<sup>50</sup> Institut für Hochenergiephysik, Österr. Akad. d. Wissensch., Nikolsdorfergasse 18, A-1050 Vienna, Austria  
<sup>51</sup> Inst. Nuclear Studies and University of Warsaw, Ul. Hoza 69, PL-00681 Warsaw, Poland  
<sup>52</sup> Fachbereich Physik, University of Wuppertal, Postfach 100 127, D-5600 Wuppertal 1, Germany

Received 14 October 1993

**Abstract.** The study of the properties of inclusive production of  $D_s$  mesons and of events in which a  $\phi$  and a muon are present in the same jet provides two independent measurements of the probability,  $f_s^w$ , for a heavy quark to hadronize into a strange  $B$  or  $D$  meson. The data sample analysed corresponds to 243,000 hadronic  $Z^0$  decays. The combined value of these measurements is  $f_s^w = 0.19 \pm 0.06 \pm 0.08$ . From the flight distance distributions of  $D_s$  and of ( $\phi$ -lepton) secondary vertices, with the lepton emitted at high transverse momentum relative to the jet axis, two values are obtained for the  $B_s^0$  meson lifetime. Combining these measurements with a previous result based on the study of  $D_s - \mu$  events, the  $B_s^0$  meson lifetime is measured to be:  $0.96 \pm 0.37$  ps.

in which a muon and a  $D_s$  meson were present in the same jet. The muon was required to have large transverse momentum ( $p_t^l$ ) relative to the jet axis, and, as a consequence, the sample was enriched in direct  $B$ -hadron semileptonic decays. The  $D_s$  meson, exclusively reconstructed through the  $\phi\pi$  or  $\bar{K}^{*0}K$  decay modes, signalled the  $B_s^0$ .

To increase statistics, two more inclusive decay channels have been used for the present analysis. Since the presence of a  $D_s$  meson provides an enriched  $B_s^0$  sample, the first consists of events containing a  $D_s$  meson decaying to  $\phi\pi$ . The second sample contains events with a high  $p_t^l$  lepton accompanied by a  $\phi$  meson in the same jet.

In Sect. 2, a description of the components of the DELPHI detector which are used in this analysis is given. The inclusive production of  $D_s$  meson and of ( $\phi$ -lepton) events are treated in Sects. 3 and 4 respectively.

Since these studies are based on samples of events rich in strange  $D$  or  $B$  hadrons, the measured rate of the selected events is used to evaluate the probability,  $f_s^w$ , that a weakly decaying strange heavy meson is produced during the hadronization process of a  $c$  or a  $b$  quark. Throughout this paper this parameter is assumed to have the same value for the two flavours of heavy quarks. It differs from the usual probability,  $f_s$ , that a heavy quark hadronizes with a strange antiquark because of the possible production of  $D_s^{**}$  or  $B_s^{0**}$  states that could decay into non-strange  $D$  or  $B$  mesons (non-strange  $D^{**}$  or  $B^{**}$  states can conversely decay into  $D_s$  or  $B_s$  mesons). Also  $f_s^w$  is more directly related to the measurements and is independent of the modelling of the hadronization mechanism. Similarly,  $f_{\text{baryon}}^w$  is the probability that a weakly decaying heavy baryon be produced by the hadronization of a heavy flavour quark.

The two selected samples of events have also been used to measure the  $B_s^0$  meson lifetime.

## 1 Introduction

In this article a study of strange  $B$  meson production in 243,000 hadronic  $Z^0$  decays recorded in the DELPHI detector in 1991 is reported. Using two independent inclusive channels, the  $B_s^0$  production rate and the decay lifetime have been measured. The study of  $B_s^0/\bar{B}_s^0$  oscillations, providing important constraints on the CKM matrix elements and leading to a measurement of the phase responsible for  $CP$  violation, will become possible when the available statistics are considerably greater than at present.

$B_s^0$  mesons are expected to be produced at a rate an order of magnitude smaller than non-strange  $B$  mesons; thus decay channels which allow strong rejection against non-strange  $B$ -hadrons have to be used. In a recent publication [1] evidence has been given for the production of  $B_s^0$  mesons at LEP from the observation of seven events

## 2 The detector

The components of the DELPHI detector which play an important role in the present analysis are described here. A complete description of the DELPHI apparatus is given in [2].

The muon identification relies mainly on the muon detector, a set of drift chambers (each with 2 layers) providing three dimensional information. In the barrel part three sets of chambers (MUB) cover polar angles between  $52^\circ$  and  $128^\circ$ , with the first located inside the magnet return yoke, the second set just outside the yoke, and the third set further out having a small overlap with the others. The two sets of forward muon chambers (MUF) cover polar angles between  $9^\circ$  and  $43^\circ$  and between  $137^\circ$  and  $171^\circ$ . In each arm the first set is located inside the yoke and the second outside.

The central tracking system, comprising the inner detector (ID), the time projection chamber (TPC) and the outer detector (OD), measures the charged particle tracks at polar angles between  $30^\circ$  and  $150^\circ$  with a resolution of  $\sigma(p)/p \simeq 0.0013 \times p$ , ( $p$  in GeV/c). The TPC, the main tracking device, is a cylinder of 30 cm inner radius, 122 cm outer radius and length 2.7 m. For the polar angles between  $39^\circ$  and  $141^\circ$  it provides up to 16 space points along the charged particle trajectory. The energy loss ( $dE/dX$ ) for each charged particle is measured by the 192 TPC sense wires as the truncated mean of the smallest 80% of the wire signals. Using  $Z^0 \rightarrow \mu^+ \mu^-$  events, the  $dE/dX$  resolution has been measured to be 5.5%. For particles in hadronic jets the resolution is 7.5%, and for 25% of the particles the  $dE/dX$  is not measured due to the presence of another charged particle within the two-track resolution distance in  $z$  of the TPC.

The Microvertex detector (VD) [3] is made of three concentric shells of silicon-strip detectors at radii of 6.3, 9 and 11 cm covering the central region of the DELPHI apparatus at polar angles between  $27^\circ$  and  $153^\circ$ . The shells surround the beam pipe, a beryllium cylinder 1.45 mm thick with a 5.3 cm inner radius. Each shell consists of 24 modules with about 10% overlap in azimuth between the modules. Each module holds 4 detectors with strips parallel to the beam direction. The silicon detectors are 300  $\mu\text{m}$  thick and have a diode pitch of 25  $\mu\text{m}$ . The read-out strips (50  $\mu\text{m}$  pitch) are AC-coupled and give a 5  $\mu\text{m}$  intrinsic precision on the coordinates of the charged particle tracks, transverse to the beam direction. After a careful procedure of relative alignment of each single detector, an overall precision of 8  $\mu\text{m}$  has been achieved. Using the combined information from OD, TPC, ID and VD a resolution of 3.5% on  $\sigma(p)/p$  has been obtained for 45 GeV/c muons.

## 3 Inclusive $D_s$ meson production

### 3.1 $D_s$ production in $Z^0$ decays

The decay of a  $B$  meson usually yields a charmed hadron. The simplest way to represent this process is by the spectator quark model where the  $b$  to  $c$  transition occurs via

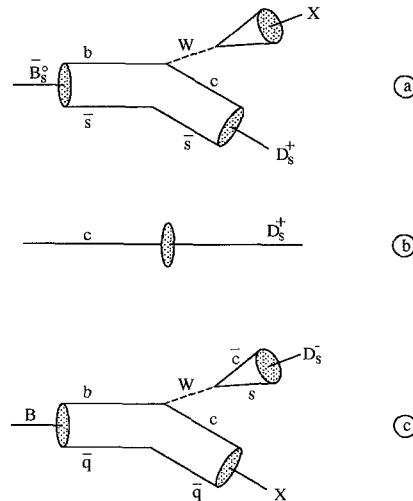


Fig. 1a-c. Quark diagrams contributing to inclusive  $D_s$  meson production

the emission of a virtual  $W$  which couples to a lepton anti-neutrino or a  $\bar{u}d$  pair. The resultant  $c$  quark recombines with the spectator antiquark to form a  $D$  meson. The corresponding diagram (Fig. 1a) shows a  $B_s^0$  meson decaying to a  $D_s$  with either a charged lepton anti-neutrino pair or light meson(s). Other  $B$ -meson decay diagrams also contribute and have been included in the version of the JETSET 7.3 generator [4] program presently used in DELPHI. The branching ratios of the  $B$  decays have been tuned to reproduce the measured inclusive decay properties of  $B^0$  and  $B^+$  mesons. According to this simulation program, which uses the same type of decay mechanisms for all  $B$  hadrons, the inclusive branching fraction  $\text{BR}(B_s^0 \rightarrow D_s X)$  is 70%, which agrees with a theoretical calculation giving  $\text{BR}(B_s^0 \rightarrow D_s X) = 86_{-13}^{+8}\%$  [5]. The latter value has been used in this analysis.

There are, however, other sources of  $D_s$  mesons in  $Z^0$  decays: the hadronization of charm quarks coming directly from the  $Z^0$  (Fig. 1b) and the decays of non-strange  $B$ 's which produce a  $D_s$  mainly in the quasi two-body process  $B \rightarrow D^{(*)} D_s^{(*)}$  (Fig. 1c). The purity of  $B_s^0$  in a  $D_s$  sample will therefore depend both on the relative strength of these different sources and on the experimental selection procedure.

Initial estimates of the branching ratios for the processes illustrated in Fig. 1 have been made by assuming that

- the couplings of the  $Z^0$  to  $c\bar{c}$  and  $b\bar{b}$  quarks pairs agree with the Standard Model expectation  $\left( \frac{\Gamma_{Z^0 \rightarrow c\bar{c}}}{\Gamma_{Z^0 \rightarrow \text{Hadrons}}} = 0.171 \text{ and } \frac{\Gamma_{Z^0 \rightarrow b\bar{b}}}{\Gamma_{Z^0 \rightarrow \text{Hadrons}}} = 0.217 \right)$ ,
- the hadronization of  $c$  and  $b$  quarks into heavy hadrons is given by the JETSET 7.3 generator program ( $f_s^w = 0.12$ ,  $f_{\text{baryon}}^w = 0.08$ ,  $\text{Prob}(b \rightarrow B_{u,d}) = 0.8$ ) and
- the production of  $D_s$  mesons in  $B^-$  or  $B_d^0$  decays is the same as the one measured in  $\Upsilon(4S)$  decays ( $\text{BR}(B_{u,d}^- \rightarrow D_s X) = 10.0 \pm 2.0(\text{stat}) \pm 4.0(\text{syst})\%$  [6]),

obtaining:

$$\text{BR}(Z^0 \rightarrow B_s^0 \rightarrow D_s X) = \frac{\Gamma_{Z^0 \rightarrow b\bar{b}}}{\Gamma_{Z^0 \rightarrow \text{Hadrons}}} \times 2 \times f_s^w \times \text{BR}(B_s^0 \rightarrow D_s X) = 4.5\%,$$

$$\text{BR}(Z^0 \rightarrow c\bar{c} \rightarrow D_s X) = \frac{\Gamma_{Z^0 \rightarrow c\bar{c}}}{\Gamma_{Z^0 \rightarrow \text{Hadrons}}} \times 2 \times f_s^w = 4.1\%,$$

$$\begin{aligned} \text{BR}(Z^0 \rightarrow B_{u,d} \rightarrow D_s X) &= \frac{\Gamma_{Z^0 \rightarrow b\bar{b}}}{\Gamma_{Z^0 \rightarrow \text{Hadrons}}} \times 2 \times (1 - f_s^w - f_{\text{baryon}}^w) \\ &\times \text{BR}(B_{u,d} \rightarrow D_s X) = 3.5\%. \end{aligned}$$

Hereafter  $D_s$  mesons produced in the process of Fig. 1b will be referred to as direct  $D_s$  and those coming from the processes of Figs. 1a and c as cascade  $D_s$ .

Using the kinematical cuts described below for selecting events with a  $D_s$  meson, the contribution from direct  $D_s$  is suppressed and a sample of events enriched in  $B_s^0$  mesons is obtained.

### 3.2 Reconstruction of $D_s$ mesons

Events containing  $D_s$  mesons are selected by the decay of a  $D_s$  to  $\phi\pi$  ( $\text{BR}(D_s \rightarrow \phi\pi) = 3.0 \pm 1.0\%$  [6]) with the  $\phi$  decaying to a  $K^+K^-$  system. The narrow width (4.4 MeV) of the  $\phi$  meson and its position (1020 MeV), close to threshold, in the  $K^+K^-$  mass distribution ensure a low combinatorial background. The spatial and the momentum resolutions of charged particles reconstructed in the

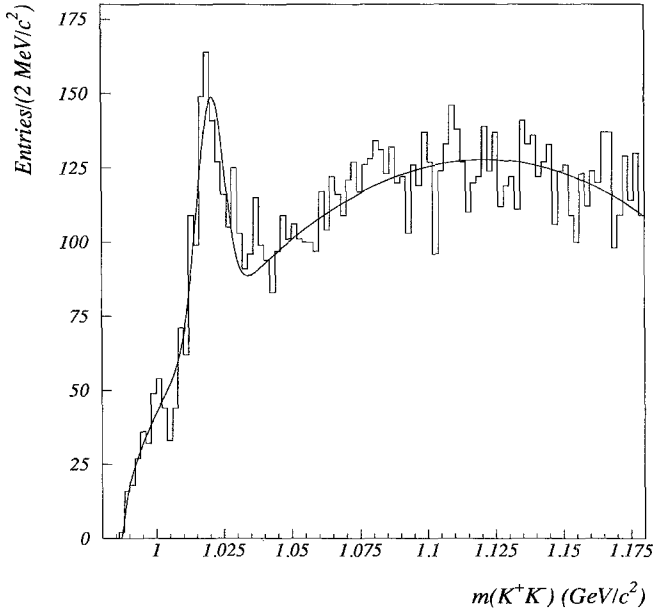


**Fig. 2.**  $K^+K^-$  mass distribution for particles with momentum greater than 2 GeV/c and measured ionization in the TPC consistent with that of a kaon. The curve shows the result of a fit with a Gaussian and a term for the background. The latter has been parametrized with the function  $B(m) = p_1 m^{p_2} (1 + p_3 m + p_4 m^2)$ , where  $m = m(KK) - 2m_K$

central tracking detector are considerably improved when the reconstructed trajectory can be associated to points measured in the vertex detector. Only particles with momentum greater than 1 GeV (0.5 GeV for the candidate pion) with at least two associated hits in the VD and having an impact parameter with respect to the fitted primary vertex less than 2 mm in the transverse plane are used in the analysis.

The invariant mass of pairs of oppositely charged particles is computed with each particle assigned the kaon mass and with the requirement that the ionisation in the TPC for each track be either unmeasured or lower than the one expected for a pion of the same momentum.

For illustration purposes in Fig. 2 the  $K^+K^-$  mass spectrum is shown for particles passing a stronger cut on the ionization, namely requiring that the ionization be measured and smaller than 90% of that expected for a pion of the same momentum. The  $\phi$  peak is observed at  $1020.2 \pm 0.5$  MeV and has a width of  $4.6 \pm 0.5$  MeV. This mass resolution is consistent with the expected value from the Monte Carlo simulation.

Secondary vertices are reconstructed for each pair of charged particles with a  $(K^+K^-)$  mass within  $\pm 12$  MeV of the nominal  $\phi$  mass with a third charged particle (assumed to be a pion) in the same jet. The 3-prong combination is retained as a  $D_s$  candidate if

- the vertex  $\chi^2$  probability is greater than 1%;
- the distance, projected in the plane perpendicular to the beam, from the primary interaction point is larger than the experimental error on the flight path (typically 300  $\mu\text{m}$ ),
- the angle  $\psi$  between the kaon and the pion in the  $\phi$  rest frame satisfies the condition  $|\cos\psi| > 0.4$ ,
- the angle  $\theta^*$ , defined as the angle between the  $\phi$  direction in the  $D_s$  rest frame and the  $D_s$  line of flight in

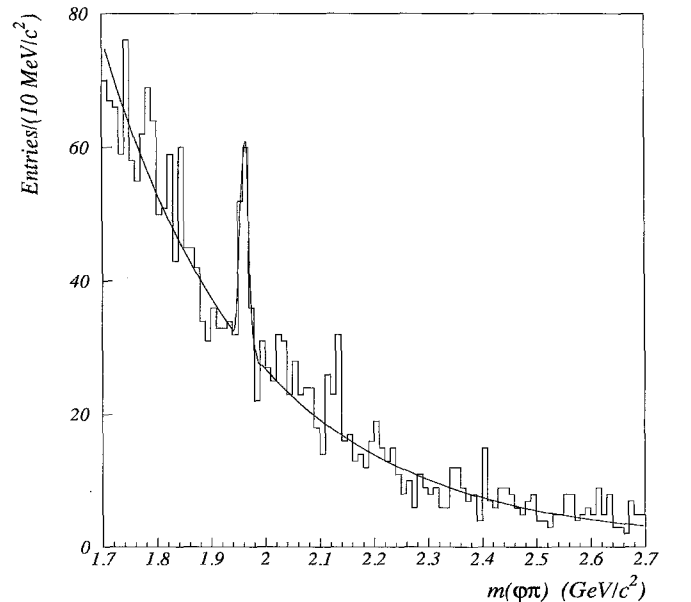


**Fig. 3.** Invariant mass distribution of the  $\phi\pi$  candidates. The curve shows the result of a fit with a Gaussian and a term for the background. The latter has been parametrized with the exponential of a second order polynomial

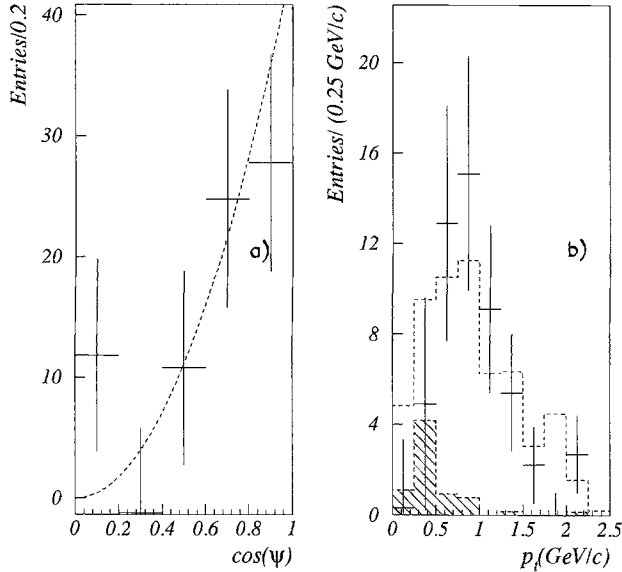


**Fig. 4.** **a**  $|\cos(\psi)|$  distribution for the events selected in the  $D_s$  signal region after combinatorial background subtraction. **b** Transverse momentum distribution of the selected  $D_s$  candidates. The Monte Carlo predictions for  $D_s$  meson production for  $b\bar{b}$  and  $c\bar{c}$  events are shown as dotted and hatched histograms respectively

the laboratory, satisfies the condition  $\cos(\theta^*) > -0.8$  and

- the fraction of the beam energy taken by a  $D_s$  meson ( $x = E_{D_s}/E_{\text{beam}}$ ) is smaller than 0.5 (this reduces the direct  $D_s$  contribution).

The resulting  $\phi\pi$  invariant mass distribution is shown in Fig. 3. A clear signal, centered at  $1962 \pm 2$  MeV, containing  $58 \pm 12$  events can be seen. This peak lies 7 MeV below the nominal  $D_s$  mass; a similar displacement has been observed by this collaboration on other reconstructed charm signals such as  $D^0 \rightarrow K^- \pi^+$  [7] and has been attributed to residual distortions in the relative alignment of individual tracking detectors.

The  $\cos(\psi)$  distribution, before the cut on this variable, has been studied to verify that the signal behaves as expected for a pseudoscalar particle decaying into a vector plus a pseudoscalar particle. The  $|\cos(\psi)|$  distribution (see Fig. 4a) after background subtraction is found to be consistent with the expected  $\cos^2(\psi)$  behaviour. The tight cut on the  $K^+ K^-$  mass has the effect of strongly suppressing contributions to the signal from kinematical reflections of other charmed mesons.

### 3.3 Measurement of $f_s^w$ from inclusive $D_s$ meson production

The efficiencies of the selection criteria are not the same for each of the processes contributing to the observed  $D_s$  meson sample. The respective contributions from the processes of Fig. 1a, b and c are different from the production rates given in Sect. 3.1. The cuts applied on the measured decay length and on the beam energy fraction taken by the  $D_s$  meson reduce the contribution from direct  $D_s$ . These efficiencies have been determined from the

Monte Carlo samples to be  $11.6 \pm 0.6(\text{stat})\%$  and  $4.7 \pm 0.8(\text{stat})\%$  for the cascade and the direct  $D_s$  meson samples, respectively, not including the branching fraction of the  $\phi$  meson into  $K^+ K^-$ .

The residual contribution of direct  $D_s$  has been studied as a function of the transverse momentum of the  $D_s$  measured with respect to the jet axis. The latter is computed using charged particles including the decay products of the  $D_s$ . This distribution, shown in Fig. 4b, has been fitted to a linear combination of the distributions for direct and cascade  $D_s$  obtained from Monte Carlo simulation. An upper limit of 9.3 events is obtained for the contribution of the direct  $D_s$  component using its fitted value increased by 1 standard deviation. This component corresponds then to less than 16% of the total number of candidates.

A consistency check of the enrichment of the sample in cascade  $D_s$  is obtained from the distribution of the apparent lifetime of the  $D_s$  defined as  $\tau_{\text{app}} = L/(\gamma\beta c \sin(\theta))$  where  $L$  is the distance, in the transverse plane, between the primary vertex and the  $D_s$  decay vertex. Selecting events with a transverse momentum larger than 0.5 GeV, the mean apparent  $D_s$  lifetime has been measured to be  $1.3 \pm 0.4$  ps. This value can be compared to the corresponding expectation from the Monte Carlo simulation of 1.5 ps for cascade and 0.6 ps for direct  $D_s$  meson production (this latter value is not equal to the true  $D_s$  lifetime because of the cut on the flight path previously described). This argument is valid if the  $B_s^0$  lifetime is not too different from the value of 1.2 ps used in the Monte Carlo simulation; this assumption is in agreement with the result obtained in this article (see Sect. 5).

The contribution of direct  $D_s$  has been computed from the production rate measured by ARGUS and CLEO [8,9] below the threshold for  $B$  meson production and from the inclusive cross-section  $\sigma(e^+e^- \rightarrow c\bar{c})$  measured at the same energy, resulting in  $\text{Prob}(c \rightarrow D_s) \text{BR}(D_s \rightarrow \phi\pi) = 0.300 \pm 0.045\%$  [9]. Assuming that this probability does not depend on the centre of mass energy, this corresponds to  $5.8 \pm 1.3$  reconstructed events which have been subtracted from the observed sample. Correcting the number of reconstructed  $D_s$  meson for the overall acceptance and efficiency and assuming the Standard Model value  $\Gamma(Z^0 \rightarrow b\bar{b})/\Gamma(Z^0 \rightarrow \text{hadrons}) = 0.217$ , the inclusive fraction of  $B$  decays to  $D_s$  mesons, subsequently decaying into  $\phi\pi$ , at LEP energies is:

$$B_1 = \text{BR}(b \rightarrow D_s X) \text{BR}(D_s \rightarrow \phi\pi) \\ = (8.5 \pm 1.9(\text{stat}) \pm 1.0(\text{syst})) \times 10^{-3}.$$

The same quantity has been measured at the  $Y(4S)$ , where no  $B_s^0$  mesons are produced, by ARGUS and CLEO collaborations [10] giving a combined value of:

$$B_2 = \text{BR}(b \rightarrow D_s X)|_{Y(4S)} \text{BR}(D_s \rightarrow \phi\pi) \\ = (2.99 \pm 0.35) \times 10^{-3}.$$

This clearly implies an excess,  $E_s$ , of inclusive  $D_s$  production in  $B$  decays at LEP. The measured excess can be

**Table 1.** Systematic errors on  $f_s^w$  determination

Systematic source	Parameter range	Absolute variation on $f_s^w$
BR ( $D_s \rightarrow \phi \pi$ )	$3 \pm 1\%$	-0.07 +0.14
BR ( $B_s^0 \rightarrow D_s X$ )	$86_{-13}^{+8}\%$	-0.03 +0.05
BR ( $b \rightarrow D_s X$ ) $_{\gamma(A,S)}$ BR ( $D_s \rightarrow \phi \pi$ )	$(2.99 \pm 0.35) \times 10^{-3}$	$\mp 0.01$
Selection efficiency	$11.7 \pm 1.3\%$	$\mp 0.04$

attributed to the production of  $D_s$  mesons in  $B_s^0$  decays and calculated from  $E_s = B_1 - (1 - f_s^w) B_2$ . Using, conservatively,  $(1 - f_s^w) = 0.8 \pm 0.2$  this excess is found to be

$$E_s = \text{BR}(b \rightarrow B_s^0 \rightarrow D_s X) \text{BR}(D_s \rightarrow \phi \pi) \\ = (6.1 \pm 1.9(\text{stat}) \pm 1.2(\text{syst})) \times 10^{-3}.$$

This measurement confirms the production of  $B_s^0$  mesons reported earlier in the study of  $D_s$  production in association with a charged lepton [1].

Alternatively the measurement of  $B_1$  and  $B_2$  together with the  $\text{BR}(D_s \rightarrow \phi \pi) = 3 \pm 1\%$  and  $\text{BR}(B_s^0 \rightarrow D_s X) = 86_{-13}^{+8}\%$  can be used to evaluate  $f_s^w$  from

$$B_1 = f_s^w \text{BR}(B_s^0 \rightarrow D_s X) \text{BR}(D_s \rightarrow \phi \pi) + (1 - f_s^w) B_2.$$

In this way the probability of a  $b$  quark fragmenting into a  $B_s^0$  meson is determined to be

$$f_s^w = 0.24 \pm 0.08(\text{stat})_{-0.09}^{+0.15}(\text{syst}).$$

The sources of the systematic error and their contributions are listed in Table 1.

The systematic uncertainty on the selection efficiency takes into account both the difference between the Monte-Carlo simulation and the actual performance of the DELPHI detector and the dependence of this efficiency on the  $B_s^0$  meson lifetime [11]. The latter effect provides the dominant contribution giving a 5% change in the selection efficiency for a 20% variation around the central value of 1.2 ps for the  $B_s^0$  meson lifetime used in the Monte Carlo.

### 3.4 A measurement of the $B_s^0$ meson lifetime

For a lifetime measurement of  $B_s^0$ , the selected sample of events has to have a high signal to background ratio. To achieve this the selection criteria described in Sect. 3.2 have been tightened, in particular those based on the TPC particle identification because they are not correlated with the variables used in this measurement. It was required that

- the ionisation information be present for both kaon candidates and be compatible, at the level of one standard deviation, with the kaon hypothesis,
- the  $K^+ K^-$  mass be within 8 MeV of the  $\phi$  mass (1020 MeV),

- the transverse momentum of the  $D_s(p_t^{D_s})$  be greater than 0.5 GeV/c.

The residual component due to direct  $D_s$  production was reduced to  $0.6 \pm 0.4$  events by the  $p_t^{D_s}$  cut. The resulting  $\phi \pi$  mass spectrum is shown in the inset of Fig. 5. In the mass interval between 1940 and 1970 MeV/c<sup>2</sup>, 17 events pass these cuts of which  $2.8 \pm 0.8$  can be attributed to the combinatorial background.

For these events a  $B$  meson proper lifetime was defined as:

$$t_B = \frac{L/(c \sin(\theta_{D_s})) - \gamma_{D_s} \beta_{D_s} \tau_{D_s}}{\gamma_B \beta_B},$$

where  $L$  is the distance between the primary vertex and the  $D_s$  decay vertex in the transverse plane.  $\gamma_B$  has been estimated using a parametrisation of the relation between  $\beta_B$  and the  $D_s$  energy. The form  $1/\gamma = a/(E_D + b) + c$  with  $a = 0.314 \pm 0.006$  GeV,  $b = -4.03 \pm 0.07$  GeV and  $c = 0.1313 \pm 0.0004$ , determined from Monte Carlo simulation, has been used. After this rescaling, the  $B_s^0$  energy resolution is found to be 21%.

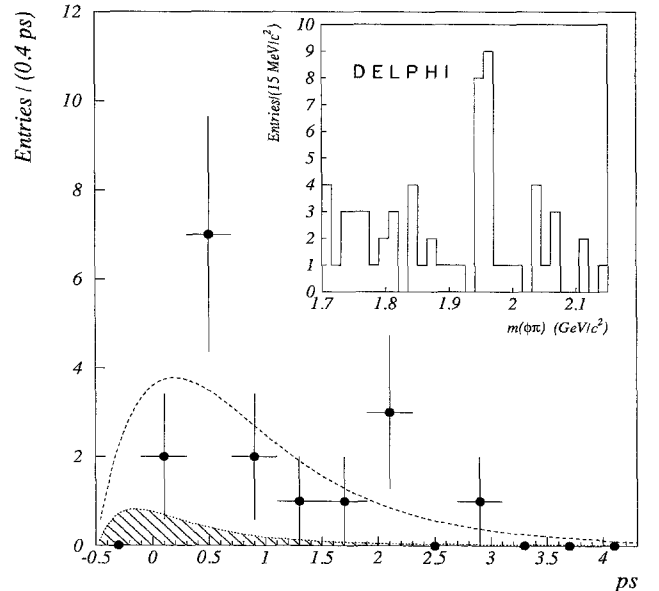


**Fig. 5.** The measured  $B$  proper time distribution for the  $D_s$  sample, shown by the points with the error bars. The curve is the result of the likelihood fit. The shaded area corresponds to the background distribution. In the inset is plotted the invariant mass distribution of the  $\phi \pi$  candidates used for the lifetime measurement after tighter selection cuts

A maximum likelihood fit has been performed on the proper decay time distribution shown in Fig. 5. The fitting function was made up of a superposition of two distributions:

- the distribution for  $B_s^0$  events, determined from Monte Carlo, taking into account the experimental resolution on the flight distance, the smearing of the estimated  $\gamma_B$  factor for  $B_s^0$  and the effect of the cut on the flight distance and
- the distribution for background, as measured from two control regions either side of the signal in the mass distribution.

The  $B$  lifetime, the only parameter of the fit, was determined to be

$$\tau(B \rightarrow D_s X) = 0.94^{+0.35}_{-0.22}(\text{stat}) \pm 0.15(\text{syst}) \text{ ps}.$$

The dominant contributions to the systematic error come from the background parametrisation and from the uncertainty on the parameters of the relation between  $\gamma_B$  and the  $D_s$  energy.

Using the combined measurement of  $f_s^w$  ( $0.19 \pm 0.10$  – see Sect. 5) presented in this article the purity in  $B_s^0$  meson of this sample is estimated to be  $71 \pm 8 \pm 6\%$ . Using the average value for the  $B$  lifetime [12] a determination of the  $B_s^0$  lifetime was obtained:

$$\tau(B_s^0) = 0.75^{+0.49}_{-0.33}(\text{stat}) \pm 0.22(\text{syst}) \text{ ps}.$$

#### 4 Inclusive associated production of $\phi$ meson and lepton

A second sample of events rich in  $B_s^0$  mesons, independent of the sample just described, has been obtained by selecting events containing a high  $p_t'$  lepton accompanied by a  $\phi$  meson in the same jet. The  $\phi$  meson is more likely to be a decay product of  $D_s$  than of non-strange charm hadrons because of the presence of a strange valence quark in the  $D_s$ . The inclusive production rate for  $\phi$  from decays of  $D^+$  and  $D^0$  due to Cabibbo suppressed transitions and also due to  $W$ -exchange diagrams for the  $D^0$ , or from final-state interactions has not been measured. Nevertheless, from the measured exclusive decay channels, it has been shown [13] that the inclusive rate of  $\phi$  mesons from  $D^0$ ,  $D^+$  and  $D_s$  meson production can be inferred with reasonable accuracy. Also, it has been shown, in Sect. 3, that the probability that a  $D_s$  meson is produced in a  $B_s^0$  meson decay is an order of magnitude larger than in non-strange  $B$  meson decays.

A sample of events with a  $\phi$  meson is thus likely to contain a mixture of  $b$  and  $c$  quark events (direct and cascade  $D_s$  events of Sect. 3). The additional requirement of an identified charged lepton in the same jet reduces the contribution of light quarks to the production of  $\phi$  mesons.

Since prompt leptons from  $B$  meson decays are emitted at larger transverse momenta than in direct charm or cascade  $B$  meson decays, selection of events with a  $\phi$  meson and a charged lepton emitted at large  $p_t'$  should provide a substantially enriched sample of  $B_s^0$  decays.

#### 4.1 Selection of $\phi$ meson-lepton events

To measure the  $B_s^0$  production rate from  $\phi$ -lepton events only muons are used. Details on muon identification are given in [14]. The identified muon is required to have associated hits in at least two layers of the VD and a measured momentum greater than 2 GeV/c.

In each event with an identified muon all other charged particle tracks with an impact parameter less than 2 mm are used to reconstruct the primary vertex using the known position of the beam spot as a constraint. If the primary vertex fit has a  $\chi^2$ -probability less than  $10^{-3}$ , an iterative procedure is applied removing, at each iteration, the track contributing most to the  $\chi^2$ . In a Monte Carlo generated  $b\bar{b}$  sample, this procedure is found to reconstruct vertices with an accuracy of 80  $\mu\text{m}$  in the horizontal direction, where the beam spot has the larger spread, and 40  $\mu\text{m}$  vertically.

Charged particles are then separated in two hemispheres by the plane orthogonal to the event thrust axis and containing the primary vertex. It has also been required that the two kaons and the lepton form a vertex with a  $\chi^2$ -probability greater than  $10^{-3}$ . The invariant mass of pairs of oppositely charged particles, assigned the kaon mass, having momentum greater than 2.5 GeV/c and in the same hemisphere as the identified muon is shown in Fig. 6a. A signal  $51 \pm 11$  events is observed centered at the expected  $\phi$  mass. Restricting the sample to events with the muon having transverse momentum greater than 1 GeV/c (to the jet axis determined without including the muon) the observed  $\phi$  signal is  $22 \pm 6$  as shown in Fig. 6b. The cut on the transverse momentum of the  $\mu$  improves the signal to noise ratio by a factor 2.

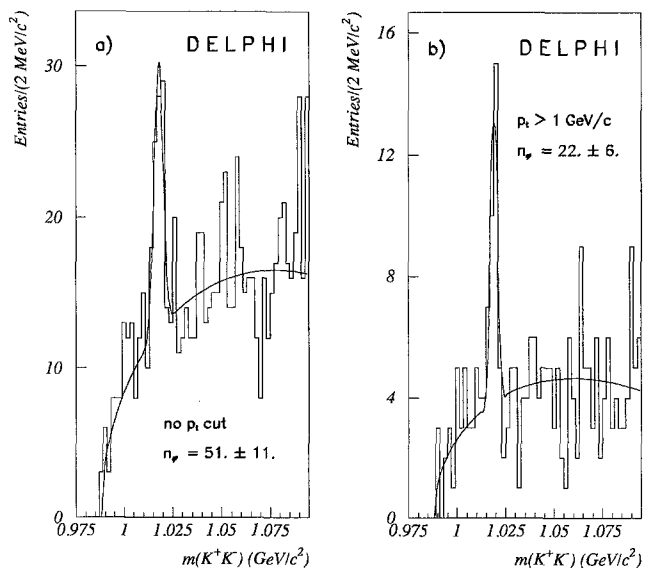


**Fig. 6a, b.**  $\phi$  meson signal in events accompanied by a muon in the same jet: **a** with no muon transverse momentum cut, and **b** with a muon transverse momentum greater than 1 GeV/c. The curves are the result of the fit of the mass spectrum using a Gaussian distribution for the signal and the same parametrization for the background as in Fig. 2

#### 4.2 Measurement of $f_s^w$ from $\phi$ meson-lepton correlations

In order to extract  $f_s^w$  from the data, the different source of signal and background have been examined. Three main processes contributing to the selected events are listed below in decreasing value of the mean transverse momentum of the muon with their probabilities per hadronic  $Z^0$  decay. The different probabilities for a given process  $I$  are noted  $P_I^x$  where the letter  $x$  refers to a subprocess which depends mainly on the strangeness content of the decaying heavy hadron. These different subprocess are displayed in Fig. 7.

● *process 1*: the muon is produced in the direct semileptonic decay of a  $B$  meson. Two processes contribute – from strange and non-strange initial  $B$  mesons (Fig. 7a):

$$P_1^a = 2 \times \left( \frac{\Gamma_{Z^0 \rightarrow b\bar{b}}}{\Gamma_{Z^0 \rightarrow \text{Hadrons}}} \right) \times f_s^w \\ \times (\text{BR}(B_s^0 \rightarrow D_s \mu X)^* \times \text{BR}(D_s \rightarrow \phi X)^* \\ + \text{BR}(B_s^0 \rightarrow D_{ns} \mu X)^* \times \text{BR}(D_{ns} \rightarrow \phi X)^*),$$

where  $D_{ns}$  means non-strange  $D$  mesons, and (Fig. 7b)

$$P_1^b = 2 \times \left( \frac{\Gamma_{Z^0 \rightarrow b\bar{b}}}{\Gamma_{Z^0 \rightarrow \text{Hadrons}}} \right) \times (1 - f_s^w - f_{\text{baryon}}^w) \\ \times (\text{BR}(B \rightarrow D^0 \mu X) \times \text{BR}(D^0 \rightarrow \phi X)^* \\ + \text{BR}(B \rightarrow D^+ \mu X) \times \text{BR}(D^+ \rightarrow \phi X)^*).$$

Non strange  $B$  meson semileptonic decay to  $D_s$  is highly suppressed since it requires a cascade  $B \rightarrow D^{**} \rightarrow D_s$  and hence has not been included.

● *process 2*: both the muon and the  $\phi$  come from a  $D$  meson produced in the cascade decay of a  $B$  meson. There are three main sub-classes:

1. the initial  $B$  meson is not strange; the  $\phi$  and the  $\mu$  are produced through decays of two different  $D$  hadrons (Fig. 7c):

$$P_2^c = 2 \times \left( \frac{\Gamma_{Z^0 \rightarrow b\bar{b}}}{\Gamma_{Z^0 \rightarrow \text{Hadrons}}} \right) \times (1 - f_s^w - f_{\text{baryon}}^w) \\ \times \text{BR}(B \rightarrow D_s D X) \\ \times (\text{BR}(D \rightarrow \mu X) \times \text{BR}(D_s \rightarrow \phi X)^* \\ + \text{BR}(D_s \rightarrow \mu X) \times \text{BR}(D \rightarrow \phi X)^*).$$

2. the initial  $B$  meson is a  $B_s^0$ ; both the  $\phi$  and the  $\mu$  are produced through the decay of a  $D_s$  meson (Fig. 7d):

$$P_2^d = 2 \times \left( \frac{\Gamma_{Z^0 \rightarrow b\bar{b}}}{\Gamma_{Z^0 \rightarrow \text{Hadrons}}} \right) \times f_s^w \\ \times \text{BR}(B_s^0 \rightarrow D_s X)^* \times \text{BR}(D_s \rightarrow \phi \mu \nu).$$

3. the initial  $B$  meson is not strange; both the  $\phi$  and the  $\mu$  are produced through the decay of a  $D_s$  meson (Fig. 7e):

$$P_2^e = 2 \times \left( \frac{\Gamma_{Z^0 \rightarrow b\bar{b}}}{\Gamma_{Z^0 \rightarrow \text{Hadrons}}} \right) \times (1 - f_s^w - f_{\text{baryon}}^w) \\ \times \text{BR}(B \rightarrow D_s X) \times \text{BR}(D_s \rightarrow \phi \mu \nu).$$

● *process 3*: the muon comes from the semileptonic decay a  $D$  meson produced in  $Z^0 \rightarrow c\bar{c}$  events (Fig. 7f). Only  $D_s$  semileptonic decays are expected to contribute to this process:

$$P_3^f = 2 \times \left( \frac{\Gamma_{Z^0 \rightarrow c\bar{c}}}{\Gamma_{Z^0 \rightarrow \text{Hadrons}}} \right) \times f_s^w \times \text{BR}(D_s \rightarrow \phi \mu \nu).$$

In these expressions it has been assumed that  $B$  baryons were not contributing to  $\phi - l$  events; this assumption gives a negligible contribution to the overall systematic uncertainty attached to the measurement of  $f_s^w$ .

In the above expressions, quantities marked by a (\*) have not been directly measured up to now and their possible ranges of variation are studied below.

The inclusive branching fractions of the  $D^0$ ,  $D^+$  and  $D_s^+$  mesons into a  $\phi$  meson have been considered in [13], and the following values are found to be most likely

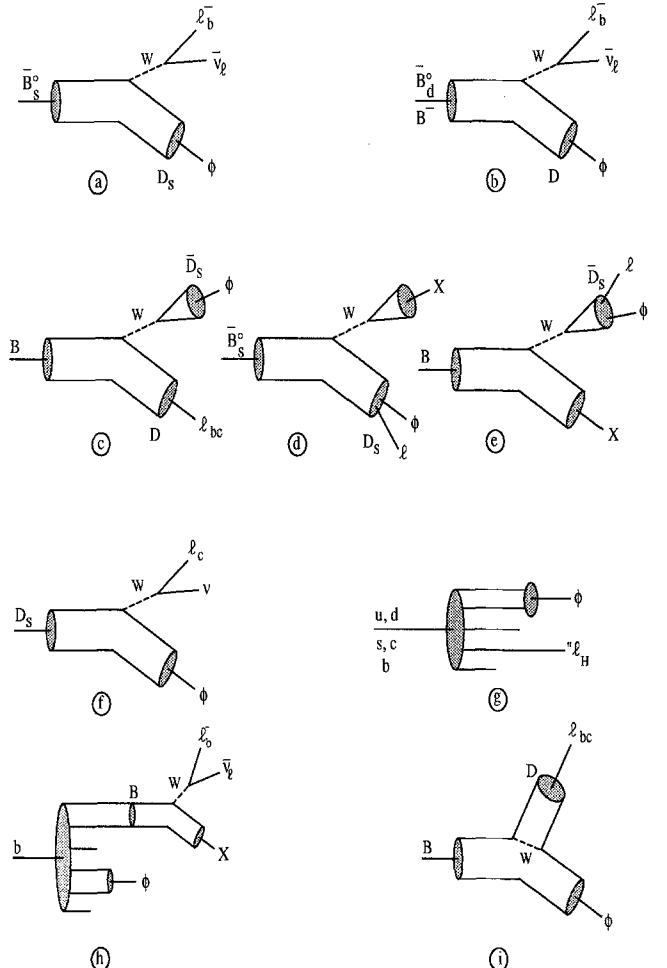


**Fig. 7a-i.** Processes contributing to the production of  $\phi - \mu$  events with the  $\phi$  and the muon appearing in the same jet. When several mechanisms of the same type contribute to a given process, only the dominant diagram has been displayed.

$$\text{BR}(D_s \rightarrow \phi X) = (4.8 \pm 0.5) \times \text{BR}(D_s \rightarrow \phi \pi^+),$$

$$\text{BR}(D^0 \rightarrow \phi X) = (1.8 \pm 0.3)\%,$$

$$\text{BR}(D^+ \rightarrow \phi X) = (1.7 \pm 0.3)\%.$$

As indicated in Sect. 3.1, the inclusive branching fraction  $B_s^0 \rightarrow D_s X$  is assumed to be  $86^{+8}_{-13}\%$ .

The probability of a  $b$  quark fragmenting to a  $B$  baryon,  $f_{\text{baryon}}^{w*}$ , is assumed to lie within 5 and 15% (set to 8% in JETSET 7.3).

The expected fractions of strange and non-strange  $D$  mesons produced in the semileptonic decays of  $B_s^0$  mesons have been inferred from the  $D^{**}$  production rate measured in non-strange  $B$  decays [15]. For the transitions  $B_s^0 \rightarrow D_s l \nu$  and  $B_s^0 \rightarrow D_s^* l \nu$ , a  $D_s$  meson is always produced in the final state, whereas in case of  $B_s^0 \rightarrow D_s^{**} l \nu$  or  $B_s^0 \rightarrow DK(n\pi) l \nu$  decays, the produced charmed meson is mainly non-strange [16]. In this analysis the following values have been used:

$$\text{BR}(B_s^0 \rightarrow D \mu X) = 10.8 \pm 0.4\%,$$

$$\text{BR}(B_s^0 \rightarrow D_s \mu X) = (0.85 \pm 0.05) \times \text{BR}(B_s^0 \rightarrow D \mu X).$$

The main sources of background have been evaluated from the Monte Carlo simulation, which has been found to describe them correctly in the analysis of inclusive muon production [14].

These are:

- events tagged by a non prompt or fake muon (the main sources are light hadron decays and hadronic punch-through) (Fig. 7g). They amount to about 40% of all the candidates. Their contribution is greater at low  $p_t^\mu$ , while for  $p_t^\mu$  greater than 1 GeV/c it amounts to  $20 \pm 7\%$  of the candidates. The contribution of this contamination has been evaluated from a Monte Carlo sample of size close to that of the data.
- events tagged by a prompt muon with the  $\phi$  meson produced as part of the original  $b$ -quark fragmentation (Fig. 7h). This contribution is expected to be small, about 5%.
- events tagged by a prompt muon with the  $\phi$  meson a decay product of the  $B$  meson and not a secondary charm particle. Contributions from non-strange  $B$  meson decays are expected to be negligible since these originate from Cabbibo suppressed transitions or non-planar hadronization mechanisms which require the presence of an  $s\bar{s}$  quark pair (Fig. 7i). In case of strange  $B$  hadron decays there could be a contribution from normal (planar) hadronization processes that require the presence of a  $s\bar{s}$

quark pair. Monte Carlo simulation suggests that this source can also be neglected.

The one remaining parameter,  $f_s^w$ , has been determined by comparing the  $p_t^\mu$  distribution to the sum of the distributions predicted from Monte Carlo simulation for the various contributing processes. The relative contribution of each predicted distribution is set equal to the central values of the branching fractions quoted above. Minimizing the  $\chi^2$  over 4  $p_t^\mu$  bins, the probability of a  $b$ -quark fragmenting to a  $B_s^0$  meson is determined to be

$$f_s^w = 0.18 \pm 0.12(\text{stat}).$$

The various contributions in the 4  $p_t^\mu$  bins are summarized in Table 2 and shown in Fig. 8.

As shown in Fig. 8a muons from direct  $B$  decays account for 80% of the candidates at transverse momenta larger than 1.2 GeV/c. In Fig. 8b the fit to the data is shown and compared with the predictions obtained for  $f_s^w = 0$  and  $f_s^w = 0.40$ .

The efficiency of the selection has been measured using a Monte Carlo sample equivalent to four times the data statistics and was found to be

$$\varepsilon(\text{direct beauty}) = 10.0 \pm 0.9\%,$$

$$\varepsilon(\text{cascade decay}) = 5.0 \pm 0.9\%,$$

$$\varepsilon(\text{direct charm}) = 6.1 \pm 1.5\%,$$

for the three classes of events. The differences in the acceptances for the different classes are mainly due to the minimum muon momentum (2.0 GeV/c) and  $\phi$  meson energy requirements.

Differences between data and Monte Carlo generated events have been investigated, the main one being due to the requirement of at least 2 VD hits associated to the muon. The efficiency of the VD cuts used to select the  $\phi - \mu$  candidates has been determined from the data, using the decay chain  $D^{*+} \rightarrow D^0 \pi^+$  where the  $D^0$  decays into  $K^- \pi^+$ . A  $D^{*+}$  signal of about 300 events is observed without any vertex detector requirement. The cuts used in selecting the  $\phi - \mu$  candidates have been applied to both data and Monte Carlo  $D^{*+}$  candidate events. Other minor differences come from the cut on the  $\chi^2$  of the secondary vertex fit and from the muon identification [14]. The efficiency determined from Monte Carlo was then corrected by the factor  $0.78 \pm 0.07$  which takes into account all these effects.

The systematic uncertainty on the value of  $f_s^w$  has been obtained by varying the parameters inside their respective acceptable range of values. The results of this study are summarized in Table 3. The total absolute variation is

**Table 2.** Number of  $\phi - \mu$  events in data and in Monte Carlo simulation

$\phi - \mu$ candidates	$p_t(0.0-0.4)$	$p_t(0.4-0.8)$	$p_t(0.8-1.2)$	$p_t > 1.2$	Processes
DATA	$12.0 \pm 7.0$	$11.0 \pm 7.7$	$11.3 \pm 6.3$	$16.7 \pm 5.7$	
MC-non-prompt muons	7.3	7.3	4.4	2.9	
MC-direct charm	4.6	1.2	0.3	0.3	$P_3^f$
MC-cascade decays	2.1	6.3	0.9	0.4	$P_2^c + P_2^d + P_2^e$
MC-direct beauty	0.6	0.8	2.7	11.6	$P_1^a + P_1^b$

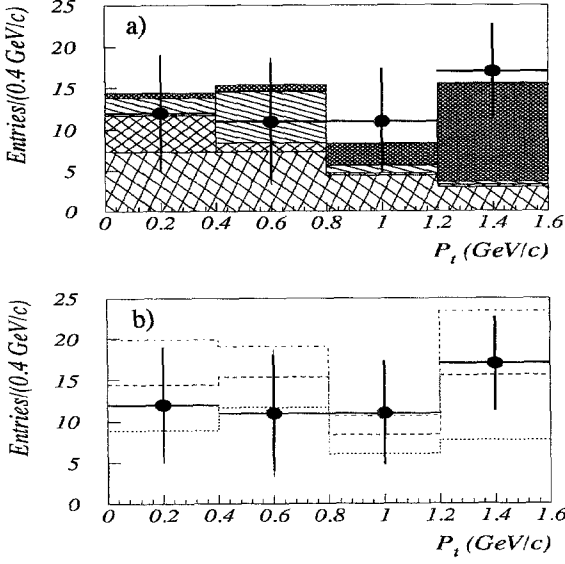


**Fig. 8a, b.** Transverse momentum distribution of the muon in  $\phi - \mu$  events. The last bin contains all events with  $p_t^\mu$  greater than 1.2 GeV/c. **a** Data (points with error bars) and contributions from (i) fake muons (cross-hatched), (ii) direct muons from  $D$  mesons (dense cross-hatched), (iii) cascade muons (diagonal hatched) and (iv) direct muons from  $B^0$  mesons (dark-hatched). **b** Data compared with expectations for different values of  $f_s^w$ : (i) 0.2 (the fit result - dashed), (ii) 0.0 (dotted), and (iii) 0.4 (dash-dotted)

0.08. The partial correlation between the branching ratio of  $D_s \rightarrow \phi \pi$  and of  $D_s \rightarrow \phi \mu \nu$  has been taken into account [16] (see first row of Table 3). The largest systematic uncertainty comes from poor knowledge of the decay branching fractions of the  $D_s$  meson. The contribution coming from all the other parameters not reported in Table 3 has been verified to be between 0.005 – 0.01. The result is

$$f_s^w = 0.18 \pm 0.12(\text{stat}) \pm 0.08(\text{syst}).$$

#### 4.3 $B_s^0$ meson lifetime

In the preceding section it has been shown that the  $B$  signal to background ratio increases as the cut on the muon transverse momentum is increased. The  $B_s^0$  lifetime measurement has, therefore, been restricted to events containing a muon with  $p_t^\mu$  greater than 1 GeV/c. To increase the statistics,  $\phi$ -electron events with  $p_t^{e1}$  greater than

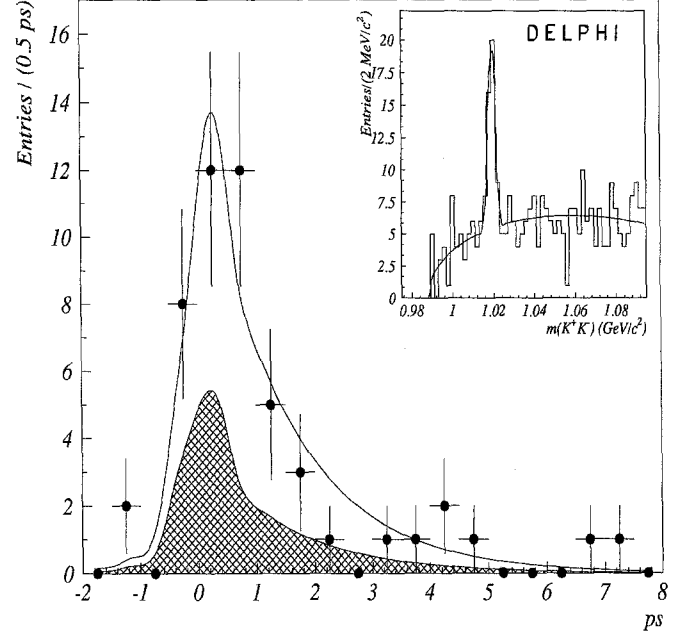


**Fig. 9.** Measured proper time distribution of  $\phi - l$  events. The curve is the result of the likelihood fit. The shaded area corresponds to the background distribution. In the inset is plotted the invariant mass distribution of the  $\phi$  candidates used for the lifetime measurement. The curve is the result of the fit of the mass spectrum using a Gaussian distribution for the signal and the same parametrization for the background as in Fig. 2

1 GeV/c have been included in the analysis. Above this  $p_t$  the purity of the identified electron sample is similar to that of the muon sample. The contamination from misidentified hadrons is at the level of 20%. The combined  $\phi$  signal contains  $31 \pm 8$  events as shown in the inset of Fig. 9, which have to be compared with the  $22 \pm 6$  events obtained with the muons alone (Fig. 6b).

Using the values of  $\phi$  meson production rate in  $D$  meson decays [13] and the probabilities for  $D^0$ ,  $D^+$ , or  $D_s^+$  meson production in  $b$  semileptonic decays [15], the purity of  $B_s^0$  in the  $\phi - l$  sample, from  $B$  decays, is determined to be

$$\frac{N_{\text{evts}}(B_s^0 \rightarrow \phi l X)}{N_{\text{evts}}(B \rightarrow \phi l X)} = 66 \pm 8(\text{stat}) + 13(\text{syst})\%.$$

In the calculation of the decay time of the  $B$  meson, two physical quantities need to be determined: the flight distance and the energy of the  $B$  meson.

**Table 3.** Systematic errors on  $f_s^w$  determination

Systematic source	Range of variation	Absolute variation of $f_s^w$
BR ( $D_s \rightarrow \phi \pi$ )	$3.0 \pm 0.7\%$	-0.06
BR ( $D_s \rightarrow \phi \mu \nu$ ) corr.	$1.5 \pm 0.3\%$	+0.04
BR ( $D_s \rightarrow \phi \pi$ )	$3.0 \pm 0.7\%$	$\mp 0.025$
BR ( $D_s \rightarrow \phi X$ )	$(4.8 \pm 0.5) \text{ BR}(D_s \rightarrow \phi \pi)$	$\mp 0.01$
DATA/MC eff. corr. factor	$78 \pm 8\%$	$\pm 0.04$
Selection efficiency:		
● Hadron misidentified	$40 \pm 8\%$	$\mp 0.03$
● Processes 1, 2, 3	$\pm 20\%$	$\mp 0.03$

The  $K^+K^-l$  pseudo-vertex is a good estimator of the  $B$  decay vertex as it has been verified using the Monte Carlo simulation. The distance ( $d_{\text{meas}}$ ) between the primary vertex and the  $K^+K^-l$  vertex has been compared with the generated  $B$  flight distance ( $d_{\text{gen}}$ ) from a sample of  $B_s^0 \rightarrow D_s \rightarrow \phi l X$  Monte Carlo generated events. The distribution of ( $d_{\text{meas}} - d_{\text{gen}}$ ) has been found to have a mean value of  $30 \mu\text{m}$  with a resolution of  $330 \mu\text{m}$  indicating that the bias introduced in determining the lifetime using  $d_{\text{meas}}$  is negligible. This result comes from the small decay distance of the  $D_s$  meson from the  $B$  decay and the small opening angle between the  $K^+$  and the  $K^-$  from the  $\phi$  decay.

The energy of the  $B$  meson has been evaluated from the momentum of the  $\phi - l$  system. A linear relation between the fraction of the  $B$  momentum carried by the  $\phi - l$  system and the momentum of the  $\phi - l$  system is observed in the Monte Carlo:

$$\frac{p(\phi l)}{p(B)} = a + b \times p(\phi l),$$

with  $a = 0.215 \pm 0.014$  and  $b = 0.018 \pm 0.005 (\text{GeV}/c)^{-1}$ .

Using this relationship the  $B$  momentum is determined with a mean resolution of 17%. The resolution improves with increasing energy of the  $\phi - l$  system. The proper decay time distribution obtained is shown in Fig. 9.

A maximum likelihood fit has been performed on the proper time distribution with the fitting function containing two terms, one describing the signal and the other the background, weighted according to their relative proportions. The proper-time distribution for the signal is obtained from an exponential convoluted with a Gaussian whose width is evaluated for each event, taking into account the accuracy on the actual vertex determination and the resolution on the  $B$  momentum. The proper-time distribution for the background has been obtained from events selected in the wings of the  $\phi$  meson signal. It contains two components, one of zero lifetime, which accounts for about 50% of the events, and one with a lifetime of 1.54 ps (arising essentially from semi-leptonic non-strange  $B$  decays). Their proper time distributions are convoluted with Gaussian distributions to account for the finite accuracy of the proper-time determination. The fraction (20%) of the events which corresponds to genuine  $\phi$  mesons associated to hadrons misidentified as leptons is assumed to have the same lifetime distribution as background events. This assumption is justified in the present situation of low statistics.

The lifetime of this sample is determined to be

$$\tau(B \rightarrow \phi l) = 1.18 \begin{matrix} +0.44 \\ -0.36 \end{matrix} (\text{stat}) \pm 0.15 (\text{syst}) \text{ ps}.$$

The systematic error is dominated by the uncertainty in the parametrisation of the background distribution and its lifetime. Using the value for the  $B_s^0$  purity of  $66\% \pm 8(\text{stat}) \begin{matrix} +13 \\ -16 \end{matrix} (\text{syst})\%$  obtained above, and taking the measured average value for the  $B$  meson lifetime [12], the  $B_s^0$  lifetime is found to be

$$\tau(B_s^0) = 1.08 \pm 0.73 \text{ ps}.$$

This result is consistent with the one recently published by OPAL [17], and with the preliminary result from ALEPH reported in [18].

## 5 Conclusions

From the measured production rates of  $D_s$  mesons and of  $\phi - \mu$  events, the probability that a  $b$  quark combines with a strange antiquark to form a strange  $B_s^0$ -meson in the hadronization process has been measured to be

$$f_s^w = 0.24 \pm 0.08(\text{stat}) \begin{matrix} +0.15 \\ -0.09 \end{matrix} (\text{syst}),$$

and

$$f_s^w = 0.18 \pm 0.12(\text{stat}) \pm 0.08(\text{syst})$$

respectively.

In both analyses the largest contributions to the systematic error come from poor knowledge of the  $D_s$  and  $B_s^0$  branching fractions. From the measurement of the production rate of  $D_s$ -lepton in the same jet [1]  $f_s^w$  was determined to be

$$f_s^w = 0.17 \pm 0.08(\text{stat}) \pm 0.06(\text{syst}).$$

Combining these three measurements the following value has been obtained:

$$f_s^w = 0.19 \pm 0.06(\text{stat}) \pm 0.08(\text{syst}).$$

From the decay time distributions, the lifetimes for the  $D_s$  and  $\phi$ -lepton samples have been measured to be

$$\tau(B \rightarrow D_s X) = 0.94 \begin{matrix} +0.35 \\ -0.24 \end{matrix} (\text{stat}) \pm 0.15 (\text{syst}) \text{ ps},$$

$$\tau(B \rightarrow \phi l \nu X) = 1.18 \begin{matrix} +0.44 \\ -0.36 \end{matrix} (\text{stat}) \pm 0.15 (\text{syst}) \text{ ps}.$$

Taking into account the purities of  $B_s^0$  in these two samples and combining them with a previous result obtained by this collaboration with  $D_s - \mu$  events [1],

$$\tau(B \rightarrow D_s l \nu X) / \tau(B) = 0.8 \pm 0.4,$$

the  $B_s^0$  meson lifetime is measured to be

$$\tau(B_s^0) = 0.96 \pm 0.37 \text{ ps}.$$

*Acknowledgements.* We are greatly indebted to our technical collaborators and to the funding agencies for their support in building and operating the DELPHI detector, and to the members of the CERN-SL Division for the excellent performance of the LEP collider.

## References

1. P. Abreu et al., DELPHI Coll.: Phys. Lett. B289 (1992) 199; see also: D. Buskulic et al., ALEPH Coll.: Phys. Lett. B294 (1992) 145; P.D. Acton et al., OPAL Coll.: Phys. Lett. B295 (1992) 357
2. P. Aarnio et al., DELPHI Coll.: Nucl. Instrum. Methods A303 (1991) 233

3. N. Binglefors et al., DELPHI Coll.: Nucl. Instrum. Methods A 328 (1993) 447
4. T. Sjöstrand: Comput Phys. Commun. 27 (1982) 243; *ibid.* 28 (1983) 229; T. Sjöstrand, M. Bengtsson: Comput. Phys. Commun. 43 (1987) 367
5. M. Suzuki: Phys. Rev. D 31 (1985) 1158
6. D.G. Cassel: in: Physics in Collision 10, p. 276. A. Goshaw, L. Montanet (eds.). Dreux: Editions Frontieres 1990
7. P. Abreu et al., DELPHI Coll.: Z. Phys. C 57 (1993) 181
8. H. Albrecht et al., ARGUS Coll.: Z. Phys. C 54 (1992) 1
9. D. Bortoletto et al., CLEO Coll.: Phys. Rev. D 37 (1988) 1719
10. D. Bortoletto et al., CLEO Coll.: Phys. Rev. Lett. 64 (1990) 2117; H. Albrecht et al., ARGUS Coll.: Z. Phys. C 54 (1992) 1
11. M. Zito: Ph.D. Thesis University Paris XI Orsay, DAPNIA/SPP 93-12 (1993)
12. P.S. Drell, J.R. Patterson: in: Proc. of the XXVI Int. Conf. on High Energy Physics, J. Sanford (ed.), Dallas (1992), vol. 1, p. 3
13. P. Roudeau, A. Stocchi: LAL 93-03 (1993)
14. P. Abreu et al., DELPHI Coll.: Z. Phys. C 56 (1992) 47
15. K. Berkelman, S.L. Stone: Ann. Rev. Nucl. Part. Sci. V41 (1991) 1
16. A. Stocchi: Ph.D. Thesis, University Paris XI Orsay, LAL 93-10 (1993)
17. P.D. Acton et al., OPAL Coll.: Phys. Lett. B 312 (1993) 425
18. F. Pierre: Report to the International Symposium on Heavy Flavour Physics, Montreal, DAPNIA/SPP 93-14 (1993)